Hexanuclear and Dodecanuclear Macrocyclic Copper(II) and Nickel(II) Complexes with Almost Planar "Benzene-like" Metal Arrays

Santokh S. Tandon,[1a] Laurence K. Thompson,*[1a] J. N. Bridson,[1a] and Cristiano Benelli[1b]

Department of Chemistry, Memorial University of Newfoundland, St. John's, Newfoundland A1B 3X7, Canada, and Inorganic Solid State Chemistry Laboratory, Department of Chemistry, University of Florence, Via Maragliano 77, Florence I-50144, Italy

Received February 24, 1995[⊗]

Template condensation of 2,6-diformyl-4-(R)phenol (R = methyl, *tert*-butyl) with 1,3-diamino-2-hydroxypropane in the presence of copper(II) and nickel(II) salts and base results in the formation of novel hexacopper(II) and hexanickel(II) complexes of the 30-membered, 3:3 macrocyclic ligands (H_6MME, H_6MTB). The macrocyclic rings contain pseudohexagonal "benzene-like" arrangements of metal centers, which are linked by alternating double (μ_2-phenoxide, μ_2-hydroxide) and single (μ_2-alkoxide) bridges within each ring: $[Cu_6(L)(\mu_2\text{-}OH)_3]_2X_6{\cdot}yH_2O$ (L = MME: X = NO_3, y = 10 (**1**); X = ClO_4, y = 6 (**2**); X = BF_4, y = 8 (**3**). L = MTB: X = ClO_4, y = 8 (**4**); X = BF_4, y = 14 (**5**)), $[Ni_6(MME)(\mu_2\text{-}OH)_3(H_2O)_6]_2X_6{\cdot}yH_2O$ (X = ClO_4, y = 4 (**7**); X = NO_3, y = 16 (**8**)). Two complexes (**1** and **4**) are dimers, with the hexagonal fragments linked by axial interactions, forming dodecanuclear species. **1** crystallized in the triclinic system, space group $P\bar{1}$, with a = 14.482(7) Å, b = 14.72(1) Å, c = 12.193(4) Å, α = 95.64(5)°, β = 92.32(4)°, γ = 114.85(4)°, and Z = 2 (R = 0.103, R_w = 0.077). Addition of NCS to the mother liquor from the preparation of **4** led to the formation of a 2:2 macrocyclic complex $[Cu(H_2MTB)(NCS)_2]_n$ (**6**). **6** crystallized in the monoclinic system, space group $P2_1/c$, with a = 12.207(2) Å, b = 14.254(3) Å, c = 9.550(3) Å, β = 95.42(2)°, and Z = 2 (R = 0.041, R_w = 0.035). The magnetic susceptibilities of **1**, **2**, **4**, **6**, **7**, and **8** were measured in the temperature range 4–305 K. The data for **1**, **2**, and **4** were analyzed and reproduced by using appropriate six-spin and twelve-spin models. For the copper derivatives, the presence of intra-ring and inter-ring antiferromagnetic interactions was determined with $-2J_1 = -2J_2$ = 318.4 cm^{-1} (**1**), $-2J_1 = -2J_2$ = 485.2 cm^{-1} (**2**), and $-2J_1 = -2J_2$ = 598.8 cm^{-1} (**4**) (six-spin model) and with $-2J_1$ = 303.8 cm^{-1}, $-2J_2$ = 262.8 cm^{-1}, $-2J_3$ = 20.0 cm^{-1} (**1**), $-2J_1$ = 484.5 cm^{-1}, $-2J_2$ = 479.0 cm^{-1}, $-2J_3$ = 16.4 cm^{-1} (**2**), and $-2J_1$ = 494.2 cm^{-1}, $-2J_2$ = 412.8 cm^{-1}, $-2J_3$ = 16.4 cm^{-1} (**4**) (twelve-spin model), while for the nickel complexes the presence of alternating ferro- and antiferromagnetic coupling was established using a six-spin model.

Introduction

Template condensation techniques involving 2,6-diformyl-4-(R)phenols (R = Me, *t*-Bu) and diamines (e.g. ethylenediamine), diamino alcohols (e.g. 1,5-diamino-3-hydroxypentane), and diaminophenols can lead to tetranuclear,[2-7] hexanuclear,[8] and octanuclear (dimers of tetranuclear species)[9,10] transition metal complexes, in which the tightly grouped metal centers are intimately bridged by phenoxide or phenoxide and alkoxide combinations. Using a longer connecting fragment, e.g. triethylenetetramine, two more distant phenoxide-bridged dinuclear copper centers combine to form a tetranuclear unit.[11] With a shorter diamino alcohol, e.g. 1,3-diamino-2-hydroxypropane, the smaller chelate ring size (5 rather than 6) leads to a situation where with 2:2 condensation four metals cannot be accommodated and with Mn(II), Ni(II), Co(II), Cu(II), Zn(II), and Cd(II) dinuclear species are formed involving N_4O_2 coordination (R = Me; R = *t*-Bu (Cu)), with phenoxide bridges linking the metal centers and no coordination of the secondary alcoholic groups.[9,12,13] In order to encourage alkoxide participation in coordination, a template reaction was carried between 2,6-diformyl-4-methylphenol and 1,3-diamino-2-hydroxypropane with copper nitrate in the presence of triethylamine, and rather than 2:2 cyclization, 3:3 cyclization occurred, with the formation of a hexanuclear macrocyclic species, which actually forms a dodecanuclear dimer. A preliminary report on the structure and some properties of $[Cu_6(MME)(\mu_2\text{-}OH)_3]_2(NO_3)_6{\cdot}10H_2O$[14] has already appeared.

In the present communication, other related copper(II) complexes will be discussed, in addition to some hexanickel complexes, and the variable-temperature magnetic properties of selected compounds will be examined using an essentially planar hexanuclear six-spin model and a model involving twelve spins. The template syntheses produce predominantly hexacopper complexes of the 3:3 macrocyclic ligands, but addition of thiocyanate in one case to the mother liquor produced a

* Author to whom correspondence should be addressed.
⊗ Abstract published in *Advance ACS Abstracts,* September 1, 1995.

(1) (a) Memorial University. (b) University of Florence.
(2) McKee, V.; Tandon, S. S. *J. Chem. Soc., Chem. Commun.* **1988**, 385.
(3) McKee, V.; Tandon, S. S. *J. Chem. Soc., Chem. Commun.* **1988**, 1334.
(4) Bell, M.; Edwards, A. J.; Hoskins, B. F.; Kachab, E. H.; Robson, R. *J. Am. Chem. Soc.* **1989**, *111*, 3603.
(5) Grannas, M. J.; Hoskins, B. F.; Robson, R. *J. Chem. Soc., Chem. Commun.* **1990**, 1644.
(6) Edwards, A. J.; Hoskins, B. F.; Kachab, E. H.; Markiewicz, A.; Murray, K. S.; Robson, R. *Inorg. Chem.* **1992**, *31*, 3585.
(7) Nanda, K. K.; Venkatsubramanian, K.; Majumdar, D.; Nag, K. *Inorg. Chem.* **1994**, *33*, 1581.
(8) Hoskins, B. F.; Robson, R.; Smith, P. *J. Chem. Soc., Chem. Commun.* **1990**, 488.
(9) McKee, V.; Tandon, S. S. *Inorg. Chem.* **1989**, *28*, 2901.
(10) McKee, V.; Tandon, S. S. *J. Chem. Soc., Dalton Trans.* **1991**, 221.
(11) Sakiyama, H.; Motoda, K-I.; Ōkawa, H.; Kida, S. *Chem. Lett.* **1991**, 1133.
(12) Tandon, S. S.; McKee, V. *J. Chem. Soc., Dalton Trans.* **1989**, 19.
(13) Tandon, S. S.; Thompson, L. K.; Bridson, J. N.; McKee, V.; Downard, A. J. *Inorg. Chem.* **1992**, *31*, 4635.
(14) Tandon, S. S.; Thompson, L. K.; Bridson, J. N. *J. Chem. Soc., Chem. Commun.* **1992**, 911.

0020-1669/95/1334-5507$09.00/0

dinuclear complex of the corresponding 2:2 macrocyclic ligand, indicating the formation of an oligomeric mixture in the template reaction.

Experimental Section

Physical Measurements. Electronic spectra were recorded as Nujol mulls using a Cary 5E spectrometer. Infrared spectra were recorded as Nujol mulls using a Mattson Polaris FT-IR instrument. Microanalyses were carried out by the Canadian Microanalytical Service, Delta, Canada. Room-temperature magnetic susceptibilities were measured by the Faraday method using a Cahn 7600 Faraday magnetic balance, and variable-temperature magnetic data (4−305 K) were obtained on dried, powdered, polycrystalline samples using an Oxford Instruments superconducting Faraday susceptometer with a Sartorius 4432 microbalance. A main solenoid field of 1.5 T and a gradient field of 10 T m^{-1} were employed.

Safety Note. Perchlorate compounds are potentially explosive and should be treated with care and in small quantities. No problems were encountered with the complexes described in this study.

Synthesis of the Complexes. $[Cu_6(MME)(\mu_2\text{-}OH)_3]_2(NO_3)_6\cdot 10H_2O$ (1), $[Cu_6(MME)(\mu_2\text{-}OH)_3]_2(ClO_4)_6\cdot 6H_2O$ (2), $[Cu_6(MME)(\mu_2\text{-}OH)_3]_2(BF_4)_6\cdot 8H_2O$ (3), $[Cu_6(MTB)(\mu_2\text{-}OH)_3]_2(ClO_4)_6\cdot 8H_2O$ (4), and $[Cu_6(MTB)(\mu_2\text{-}OH)_3]_2(BF_4)_6\cdot 14H_2O$ (5). A solution of 2,6-diformyl-4-*tert*-butylphenol (DTBP)[15,16] (0.21 g, 1.0 mmol) in methanol (20 mL) was added to a solution of $Cu(ClO_4)_2\cdot 6H_2O$ (0.74 g, 2.0 mmol) in methanol (50 mL), and the mixture was refluxed for 20 min. A solution of 1,3-diamino-2-hydroxypropane (DAHP) (0.090 g, 1.0 mmol) in methanol (40 mL) containing triethylamine (2.0 mmol) was added dropwise over a period of about 15 min. The green solution was refluxed for 24 h, filtered, and reduced in volume to ≈20 mL. On standing, a green crystalline solid (**4**) was obtained. Recrystallization from DMF/MeOH gave crystals suitable in appearance for X-ray analysis. A further crop of green product was obtained by slow evaporation of the filtrate. Yield: 60%. Excess KNCS dissolved in an EtOH/H_2O mixture was added to the remaining mother liquor, with the formation of a green crystalline solid (**6**). Anal. Calcd for $C_{45}H_{65}N_6O_{25}Cl_3Cu_6$ (**4**): C, 34.26; H, 4.15; N, 5.33. Found: C, 33.94; H, 4.03; N, 5.41. Compounds **1**−**3** and **5** were prepared similarly using DTBP or 2,6-diformyl-4-methylphenol (DFMP)[15,16] and the appropriate copper salt. Anal. Calcd for $C_{36}H_{49}N_9O_{23}Cu_6$ (**1**): C, 31.86; H, 3.61; N, 9.36. Found: C, 31.81; H, 3.21; N, 9.26. Calcd for $C_{36}H_{45}N_6O_{24}Cl_3Cu_6$ (**2**): C, 30.17; H, 3.16; N, 5.86; Cu, 26.60. Found: C, 30.20; H, 3.10; N, 5.41; Cu, 26.11. Calcd for $C_{36}H_{47}N_6O_{13}B_3F_{12}Cu_6$ (**3**): C, 30.59; H, 3.36; N, 5.95; Cu, 27.00. Found: C, 30.38; H, 3.28; N, 6.04; Cu, 27.85. Calcd for $C_{45}H_{71}N_6O_{16}B_3F_{12}Cu_6$ (**5**): C, 33.90; H, 4.30; N, 5.27. Found: C, 33.35; H, 3.84; N, 5.74.

$[Ni_6(MME)(\mu_2\text{-}OH)_3(H_2O)_6]_2(ClO_4)_6\cdot 4H_2O$ (7) and $[Ni_6(MME)(\mu_2\text{-}OH)_3(H_2O)_6]_2(NO_3)_6\cdot 16H_2O$ (8). $Ni(ClO_4)_2\cdot 6H_2O$ (1.46 g, 4.00 mmol) and DFMP (0.326 g, 2.00 mmol) were dissolved in methanol (100 mL), and the mixture was refluxed for 10 min. A solution of 1,3-diamino-2-hydroxypropane (0.180 g, 2.00 mmol) and triethylamine (0.81 g, 8.0 mmol) in methanol (20 mL) was then added dropwise over a period of 5 min. A dirty green solution formed, which was refluxed for 24 h. The solution volume was reduced to ≈20 mL, and ethanol (50 mL) was added. A brown solid precipitated, which was filtered off after standing at room temperature for 3 days. Yield: 45%. Anal. Calcd for $C_{36}H_{55}N_6O_{29}Cl_3Ni_6$ (**7**): C, 28.93; H, 3.71; N, 5.63; Ni, 23.57. Found: C, 28.53; H, 3.93; N, 5.39; Ni, 23.08. **8** was prepared similarly using nickel nitrate. Anal. Calcd for $C_{36}H_{67}N_9O_{32}Ni_6$ (**8**): C, 29.02; H, 4.52; N, 8.46; Ni, 23.64. Found: C, 28.72; H, 3.92; N, 8.00; Ni, 23.57.

All samples were dried under vacuum prior to elemental analysis, and magnetic measurements were carried out on analytically pure samples.

Crystallographic Data Collection and Refinement of the Structures. $[Cu_6(MME)(\mu_2\text{-}OH)_3]_2(NO_3)_6\cdot 10H_2O$ (1). The diffraction intensities of a deep green irregular crystal of **1** with approximate dimensions 0.35 × 0.35 × 0.20 mm were collected with graphite-monochromatized Mo Kα radiation using a Rigaku AFC6S diffractometer at 25 ± 1 °C and the $\omega-2\theta$ scan technique to a $2\theta_{max}$ value of 50.0°. A total of 8591 reflections were measured, of which 8173 (R_{int} = 0.089) were unique and 3674 were considered significant with $I_{net} > 2.0\sigma(I_{net})$. An empirical absorption correction was applied, after a full isotropic refinement, using the program DIFABS,[17] which resulted in transmission factors ranging from 0.82 to 1.00. The data were corrected for Lorentz and polarization effects. The cell parameters were obtained from the least-squares refinement of the setting angles of 13 carefully centered reflections with 2θ in the range 38.2−46.3°.

Table 1. Summary of Crystallographic Data for $[Cu_6(MME)(\mu_2\text{-}OH)_3]_2(NO_3)_6\cdot 10H_2O$ (**1**) $[Cu_2(MTB)(NCS_2]_n$ (**6**)

	1	**6**
empirical formula	$C_{38}H_{36}N_9O_{21}Cu_6$	$C_{32}H_{38}N_6S_2O_4Cu_2$
fw	1336.03	761.9
space group	$P\bar{1}$	$P2_1/c$
a (Å)	14.482(7)	12.207(2)
b (Å)	14.72(1)	14.254(3)
c (Å)	12.193(4)	9.550(3)
α (deg)	95.64(5)	
β (deg)	92.32(4)	95.42(2)
γ (deg)	114.85(4)	
V (Å^3)	2337(6)	1654(1)
ϱ_{calcd} (g cm^{-3})	1.898	1.530
Z	2	2
μ (cm^{-1})	27.78	14.55
λ (Å)	0.71069	0.710 69
T (°C)	25(1)	25(1)
R^a	0.103	0.041
R_w	0.077	0.035

^{a} $R = \sum||F_o| - |F_c||/\sum|F_o|$, $R_w = [\sum w(|F_o| - |F_c|)^2/\sum wF_o^2]^{1/2}$.

The crystals of **1** were large irregular fragments, and rather broad peaks were obtained during the *search* routine, which may have resulted from some loss of lattice solvent. Indexing was, however, successful. The structure was solved by direct methods.[18,19] Because of a generally poor data set, only the coppers and bonded oxygen atoms in the hexanuclear ring were set anisotropic during refinement. Only one nitrate group was clearly identified in the solution, and several peaks of significant intensity were assigned as lattice or coordinated water. The main hexanuclear fragment was, however, unequivocally identified, although its geometry was of somewhat limited precision. Two peaks within a reasonable bonding distance were assigned as a methanol, although, while the oxygen refined normally, the carbon had high thermal parameters. While a methanol is a reasonable solvent molecule present in the crystallographic sample, its apparent absence in the analytical sample is consistent with the fact that this sample was dried under vacuum. The final cycle of full-matrix least-squares refinement was based on 3674 observed reflections ($I > 2.00\sigma(I)$) and 380 variable parameters and converged with unweighted and weighted agreement factors of $R = \sum||F_o| - |F_c||/\sum|F_o| = 0.103$ and $R_w = [(\sum w(|F_o| - |F_c|)^2/\sum wF_o^2)]^{1/2} = 0.077$. The maximum and minimum peaks on the final difference Fourier map correspond to 1.41 and −1.30 electrons/Å^3, respectively. Neutral-atom scattering factors[20] and anomalous-dispersion terms[21,22] were taken from the usual sources. All calculations were performed with the TEXSAN[23] crystallographic software package using a VAX 3100 work station. A summary of the crystal and other data is given in Table 1, and atomic coordinates are given in Table 2.

(15) Ullman, F.; Brittner. *Chem. Ber.* **1909**, *42*, 2539.
(16) Gagné, R. R.; Spiro, C. L.; Smith, T. J.; Hamann, C. A.; Thies, W. R.; Shiemke, A. K. *J. Am. Chem. Soc.* **1981**, *103*, 4073.
(17) Walker, N.; Stuart, D. *Acta Crystallogr.* **1983**, *A39*, 158.
(18) Gilmore, C. J. *J. Appl. Crystallogr.* **1984**, *17*, 42.
(19) Beurskens, P. T. DIRDIF: Technical Report 1984/1; Crystallography Laboratory: Toernooiveld, 6525 Ed Nijmegen, The Netherlands, 1984.
(20) Cromer, D. T.; Waber, J. T. *International Tables for X-ray Crystallography*; The Kynoch Press: Birmingham, United Kingdom, 1974; Vol. IV, Table 2.2A.
(21) Ibers, J. A.; Hamilton, W. C. *Acta Crystallogr.* **1974**, *17*, 781.
(22) Cromer, D. T. *International Tables for X-ray Crystallography*; The Kynoch Press: Birmingham, United Kingdom, 1974; Vol. IV, Table 2.3.1.
(23) *Texsan-Texray Structure Analysis Package*; Molecular Structure Corp.: The Woodlands, TX, 1985.

Table 2. Final Atomic Positional Parameters and B(eq) Values (Å^2) for $[Cu_6(MME)(\mu_2\text{-}OH)_3]_2(NO_3)_6\cdot 10H_2O$ (**1**)

atom	x	y	z	B(eq)	atom	x	y	z	B(eq)[a]
Cu(1)	0.7533(2)	0.3070(2)	0.5562(2)	3.6(1)	C(18)	0.358(1)	−0.327(2)	0.164(2)	3.3(4)
Cu(2)	0.5963(2)	0.2483(2)	0.3710(2)	3.8(1)	C(19)	0.170(2)	−0.457(2)	−0.097(2)	4.4(5)
Cu(3)	0.4651(2)	−0.0125(2)	0.2717(2)	3.7(1)	C(20)	0.404(2)	−0.365(2)	0.244(2)	4.0(5)
Cu(4)	0.5021(2)	−0.1672(2)	0.3796(2)	3.7(1)	C(21)	0.504(2)	−0.359(2)	0.411(2)	4.0(5)
Cu(5)	0.6871(2)	−0.0954(2)	0.6121(2)	4.0(1)	C(22)	0.602(2)	−0.272(2)	0.462(2)	3.6(5)
Cu(6)	0.8023(2)	0.1218(2)	0.6841(2)	3.8(1)	C(23)	0.643(1)	−0.302(1)	0.562(2)	3.4(4)
O(1)	0.695(1)	0.373(1)	0.459(1)	4.0(6)	C(24)	0.797(2)	−0.204(2)	0.684(2)	5.2(6)
O(2)	0.497(1)	0.1312(8)	0.278(1)	3.2(5)	C(25)	0.879(2)	−0.020(2)	0.762(2)	3.8(5)
O(3)	0.427(1)	−0.158(1)	0.247(1)	4.1(6)	C(26)	0.879(2)	−0.114(2)	0.746(2)	3.8(5)
O(4)	0.579(1)	−0.188(1)	0.502(1)	3.8(6)	C(27)	0.960(2)	−0.129(2)	0.796(2)	4.7(5)
O(5)	0.798(1)	−0.008(1)	0.720(1)	3.9(6)	C(28)	1.041(2)	−0.050(2)	0.857(2)	3.9(5)
O(6)	0.8096(9)	0.2545(9)	0.664(1)	3.3(5)	C(29)	1.040(2)	0.039(2)	0.871(2)	4.5(5)
O(7)	0.6289(9)	0.190(1)	0.494(1)	3.3(5)	C(30)	0.963(1)	0.059(1)	0.828(1)	2.8(4)
O(8)	0.5459(9)	−0.0187(8)	0.403(1)	2.8(5)	C(31)	1.133(2)	−0.065(2)	0.906(2)	5.3(6)
O(9)	0.6705(9)	0.027(1)	0.607(1)	3.4(6)	C(32)	0.973(2)	0.160(2)	0.841(2)	4.3(5)
N(1)	0.574(1)	0.325(1)	0.262(1)	3.2(4)	C(33)	0.940(2)	0.299(2)	0.812(2)	4.6(5)
N(2)	0.389(1)	−0.025(1)	0.130(1)	3.6(4)	C(34)	0.911(2)	0.330(2)	0.706(2)	4.1(5)
N(3)	0.461(1)	−0.309(1)	0.333(1)	3.5(4)	C(35)	0.909(2)	0.429(2)	0.721(2)	4.0(5)
N(4)	0.718(1)	−0.210(1)	0.630(1)	3.3(4)	C(36)	0.872(2)	0.523(2)	0.590(2)	4.2(5)
N(5)	0.915(1)	0.191(1)	0.794(1)	3.2(4)	O(10)	0.748(1)	0.234(1)	0.280(1)	7.5(5)
N(6)	0.851(1)	0.440(1)	0.623(1)	3.0(3)	O(11)	0.866(1)	0.309(1)	0.420(2)	8.1(5)
C(1)	0.737(2)	0.465(2)	0.432(2)	3.4(5)	O(12)	0.904(2)	0.292(2)	0.255(2)	12.5(8)
C(2)	0.824(1)	0.540(2)	0.497(2)	3.3(4)	N(7)	0.841(2)	0.271(2)	0.323(2)	9.0(7)
C(3)	0.859(2)	0.635(2)	0.471(2)	4.6(5)	O(13)	0.820(2)	−0.020(2)	0.445(2)	15.7(9)
C(4)	0.820(2)	0.663(2)	0.387(2)	4.6(5)	O(14)	0.892(1)	0.119(1)	0.522(2)	9.2(5)
C(5)	0.741(2)	0.589(2)	0.319(2)	4.7(5)	O(15)	0.780(3)	0.078(3)	0.379(4)	13(1)
C(6)	0.697(2)	0.488(2)	0.339(2)	4.1(5)	O(16)	0.629(1)	0.024(1)	0.179(1)	9.0(5)
C(7)	0.861(2)	0.770(2)	0.364(2)	7.1(7)	O(17)	0.965(4)	0.029(4)	0.462(4)	15(2)
C(8)	0.617(2)	0.420(2)	0.258(2)	4.5(5)	O(18)	0.673(1)	−0.116(1)	0.260(2)	5.9(5)
C(9)	0.493(2)	0.254(2)	0.174(2)	5.1(6)	C(37)	0.635(7)	−0.160(7)	0.161(7)	31(2)
C(10)	0.492(2)	0.154(2)	0.167(2)	3.9(5)	O(19)	0.026(2)	0.345(2)	0.076(2)	15.8(9)
C(11)	0.395(1)	0.072(2)	0.108(2)	3.6(5)	O(20)	0.205(5)	0.303(4)	0.005(5)	13(2)
C(12)	0.338(1)	−0.104(2)	0.064(2)	3.5(5)	O(21)	0.162(5)	0.335(5)	0.052(5)	15(2)
C(13)	0.370(1)	−0.228(2)	0.165(2)	3.3(4)	O(22)	0.202(2)	0.383(2)	0.188(2)	14.1(8)
C(14)	0.327(1)	−0.200(1)	0.076(1)	2.6(4)	O(23)	0.346(3)	0.388(3)	0.178(3)	20(1)
C(15)	0.265(1)	−0.276(2)	−0.007(1)	3.1(4)	N(8)	0.246(3)	0.320(3)	0.098(4)	18(1)
C(16)	0.246(1)	−0.373(2)	−0.008(2)	3.6(5)	O(24)	0.349(3)	0.288(3)	0.898(3)	22(1)
C(17)	0.295(2)	−0.397(2)	0.076(2)	4.2(5)	O(25)	0.473(4)	0.486(4)	0.953(3)	21(2)

[a] $B(\text{eq}) = (8\pi^2/3)\sum_{i=1}^{3}\sum_{j=1}^{3} U_{ij} a_i^* a_j^* \vec{a}_i \cdot \vec{a}_j$.

Hydrogen atomic coordinates (Table S1), anisotropic thermal parameters (Table S2), and a full listing of bond distances and angles (Table S3) are included as Supporting Information.

$[Cu_2(H_2MTB)(NCS)_2]_n$ (6). The crystals of **6** are green, diamond-like plates. The diffraction intensities of an approximately 0.35 × 0.35 × 0.08 mm crystal were collected with graphite-monochromatized Mo Kα radiation using a Rigaku AFC6S diffractometer at 26 ± 1 °C and the $\omega-2\theta$ scan technique to a $2\theta_{max}$ value of 50.0°. A total of 3237 reflections were measured, of which 3048 (R_{int} = 0.146) were unique and 1663 were considered significant with $I_{net} > 3.0\sigma(I_{net})$. An empirical absorption correction was applied, after a full isotropic refinement, using the program DIFABS,[17] which resulted in transmission factors ranging from 0.84 to 1.00. The data were corrected for Lorentz and polarization effects. The cell parameters were obtained from the least-squares refinement of the setting angles of 25 carefully centered reflections with 2θ in the range 27.4−32.6°.

The structure was solved by direct methods.[18,19] All atoms except hydrogens were refined anisotropically. Hydrogen atoms were included in calculated positions, except in the region of C(14) and the disordered secondary alcohol. Three of the four were located from difference maps, and one on C(14) was calculated. For calculated hydrogens, isotropic thermal parameters were set at 20% greater than those of their bonded partners. Hydrogens were included, but not refined, in the final rounds of least-squares. The final cycle of full-matrix least-squares refinement was based on 1663 observed reflections ($I > 3.00\sigma(I)$) and 218 variable parameters and converged with unweighted and weighted agreement factors of $R = \sum||F_o| - |F_c||/\sum|F_o| = 0.041$ and $R_w = [(\sum w(|F_o| - |F_c|)^2/\sum wF_o^2)]^{1/2} = 0.035$. The maximum and minimum peaks on the final difference Fourier map correspond to 0.34 and −0.43 electron/Å^3, respectively. Neutral-atom scattering factors[20] and anomalous-dispersion terms[21,22] were taken from the usual sources. All calculations were performed with the TEXSAN[23] crystallographic software package using a VAX 3100 work station. A summary of the crystal and other data is given in Table 1, and atomic coordinates are given in Table 3. Hydrogen atomic coordinates (Table S4), anisotropic thermal parameters (Table S5), and a full listing of bond distances and angles (Table S6) are included as Supporting Information.

Results and Discussion

Description of the Structures of $[Cu_6(MME)(\mu_2\text{-}OH)_3]_2(NO_3)_6\cdot 10H_2O$ (1) and $[Cu_2(H_2MTB)(NCS)_2]_n$ (6). The structure of **1** is illustrated in Figures 1 and 2, and distances and angles relevant to the copper coordination spheres are given in Table 4. The problems associated with locating three nitrates in the structure bring into question the charge carried by oxygens O(7), O(8), and O(9). Elemental analysis is, however, entirely consistent with the presence of three nitrates, indicating that these oxygens are in fact hydroxides. Figure 1 shows the hexanuclear fragment with the hexagonal arrangement of the six pseudo-square-planar copper(II) centers, which are bridged alternately by the μ_2-hydroxide and μ_2-phenoxide pair and the μ_2-alkoxide. The copper atoms themselves are consequently linked by alternate short (Cu−Cu 2.927−2.960 Å; double) and long (Cu−Cu 3.547−3.571 Å; single) contacts, in an arrangement that is analogous, in a sense, to a resonance form of benzene. The chelate rings at the phenolic groups are six-membered, while the alkoxide bridges generate five-membered chelate rings. The net effect of the alternating 6,6,5,5 chelate ring arrangement is to establish a fairly flat hexagonal ring of copper centers, with equatorial copper−oxygen and copper−nitrogen bonds that are all quite short (1.91−1.98 Å) (Cu

Table 3. Final Atomic Positional Parameters and B(eq) Values (Å^2) for $[Cu_2(H_2MTB)(NCS)_2]_n$ (**6**)

atom	x	y	z	B(eq)[a]
Cu(1)	0.49293(6)	−0.42710(5)	−0.12050(7)	2.38(3)
S(1)	0.7366(2)	−0.4017(1)	−0.4329(2)	6.4(1)
O(1)	0.5890(3)	−0.4686(2)	0.0440(3)	2.1(2)
O(2)	0.4028(6)	−0.1672(5)	−0.4044(7)	3.6(4)
O(3)	0.3602(6)	−0.2162(6)	−0.2200(8)	2.9(4)
N(1)	0.5816(4)	−0.3145(3)	−0.1494(4)	2.0(2)
N(2)	0.3773(4)	−0.4040(3)	−0.2697(4)	2.4(2)
N(3)	0.6036(5)	−0.5165(4)	−0.2839(6)	4.3(3)
C(1)	0.6928(4)	−0.4418(4)	0.0797(5)	1.8(2)
C(2)	0.7414(4)	−0.3680(4)	0.0088(5)	2.0(2)
C(3)	0.8503(4)	−0.3425(4)	0.0499(5)	2.4(3)
C(4)	0.9150(4)	−0.3840(4)	0.1576(5)	2.2(3)
C(5)	0.8652(4)	−0.4534(4)	0.2286(5)	2.7(3)
C(6)	0.7568(4)	−0.4839(4)	0.1926(5)	2.1(3)
C(7)	1.0355(5)	−0.3533(5)	0.1957(6)	3.3(3)
C(8)	1.0809(6)	−0.3907(6)	0.3385(8)	6.1(4)
C(9)	1.0444(6)	−0.2468(5)	0.2032(9)	6.3(5)
C(10)	1.1051(6)	−0.3913(6)	0.0848(8)	7.2(5)
C(11)	0.6830(4)	−0.3083(4)	−0.0981(5)	2.1(2)
C(12)	0.7174(4)	−0.5552(4)	0.2807(5)	2.4(3)
C(13)	0.5481(5)	−0.2385(4)	−0.2515(6)	2.8(3)
C(14)	0.4291(5)	−0.2417(4)	−0.3108(6)	2.7(3)
C(15)	0.3973(5)	−0.3343(4)	−0.3772(6)	2.9(3)
C(16)	0.6599(5)	−0.4701(4)	−0.3466(6)	3.5(3)

[a] $B_{(eq)} = (8\pi^2/3)\sum_{i=1}^{3}\sum_{j=1}^{3} U_{ij} a_i^* a_j^* \vec{a}_i \cdot \vec{a}_j$.

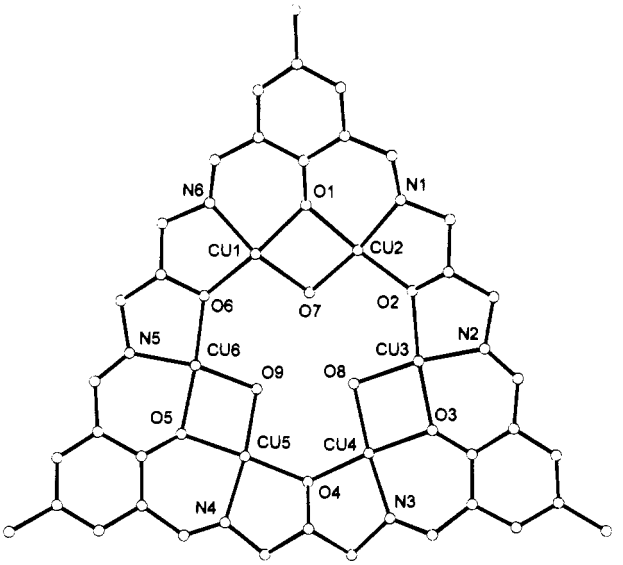

Figure 1. Structural representation of one hexanuclear ring for $[Cu_6(MME)(\mu_2\text{-}OH)_3]_2(NO_3)_6 \cdot 10H_2O$ (**1**) (hydrogen atoms omitted).

deviations from the Cu_6 plane are <0.03 Å). The Cu−N and Cu−O distances are normal for macrocyclic ligands of this sort,[9,10,24] but the essentially planar hexacopper array is unique. A measure of the deviation from macrocyclic planarity can be seen in the sums of the angles around the alkoxide bridges (O(2) 349.6°, O(4) 350.0°, O(6) 352.2°) and the phenoxide bridges (O(1) 354.1°, O(3) 359.8°, O(5) 352.1°), which in most cases are somewhat less than the idealized value of 360°. A comparable Cu_6 complex of a more flexible macrocyclic ligand derived from the template condensation of DFMP and 2,6-bis-(aminomethyl)-4-methylphenol in the presence of copper acetate, leads to a "cyclohexane boat" arrangement of six copper(II) centers, which can be associated with the presence of a 6,6,6,6 arrangement of chelate rings.[8] The oxygen bridge angles in **1** vary widely, in keeping with the difference in chelate ring sizes. Cu−O(alkoxide)−Cu bridge angles fall in the range 131.6−135.2°, while Cu−O(phenoxide)−Cu and Cu−O(hydroxide)−Cu bridge angles fall in the ranges 96.1−97.8° and 96.4−98.4°, respectively. The central cavity of each macrocyclic ring is occupied by the three hydroxides, with an asymmetric triangular arrangement of oxygen atoms. The O(7)−O(9) contact (3.13-(2) Å) is significantly longer than the other two (O(7)−O(8) 2.86(2) Å, O(8)−O(9) 2.86(1) Å), which is consistent with the fact that both O(7) and O(9) are involved in equatorial contacts to the adjacent metallacyclic ring.

The hexanuclear macrocyclic rings are dished slightly and coupled together via their convex faces (Figure 2) by two of the hydroxide oxygens (O(7), O(9)), which act as μ_3 linkages connecting Cu(1) and Cu(2) on one ring with Cu(4′) on the other and Cu(5) and Cu(6) on one ring with Cu(3′), respectively, on the other. The molecular symmetry dictates that this intermacrocyclic bridging also involves symmetry-related atoms, and so the two rings are held together by four axial hydroxide bridges in the dodecanuclear structural arrangement. The inter-ring contacts are relatively short (Cu(3′)−O(9) 2.45(1) Å, Cu-(4′)−O(7) 2.43(1) Å), indicating a significant axial interaction at O(7) and O(9). A pair of symmetry-related, bidentate nitrate groups, bonded to Cu(1) via O(11) and to Cu(2) via O(10), are located on the outer (concave) face of the complex (Cu(1)−O(11) 2.37(2) Å, Cu(2)−O(10) 2.58(2) Å). A second pair of oxygen atoms are bonded axially on the outer face to Cu(5) and Cu(6) (not shown; Cu(5)−O(13) 2.83(3) Å, Cu(6)−O(14) 2.42(2) Å) and are assumed to be part of a second bidentate nitrate. However, although a third reasonably placed oxygen (O(17)) could be located, the central nitrogen could not be located successfully in the Fourier map. A methanol molecule (C(37)) is coordinated weakly in an axial, external fashion to Cu(4) (Cu(4)−O(18) 2.78(2) Å), and a water molecule is bound similarly to Cu(3) (Cu(3)−O(16) 2.54(2) Å). A preliminary structure determination of **4** shows a similar dodecanuclear arrangement with four relatively short hydroxide contacts linking the hexanuclear halves. Angles at the alkoxide oxygen are comparable with **1**, but the hydroxide and phenoxide bridge angles are somewhat larger.

The structure of **6** is illustrated in Figure 3, and distances and angles relevant to the copper coordination spheres are given in Table 5. The dinuclear complex involves the coordination of two copper(II) centers in the normal manner for a 2:2 macrocyclic ligand of this sort, with the two phenoxide groups bridging the two metals. The secondary alcohol group is not coordinated within the macrocyclic complex itself and adopts an exo-ring conformation with the oxygen atom disordered over two positions (O(2), O(3)), a feature which has been observed before in comparable complexes.[13] The Cu−Cu separation (3.094 Å) and Cu−O−Cu angle (103.8(2)°) are somewhat larger than similar dimensions in **1** but typical for dinuclear, 2:2 macrocyclic complexes with three-carbon linkers between the azomethine nitrogen atoms.[13,25−27] The copper centers are bound by four in-plane ligand atoms with short contacts (<1.98 Å), and a weakly bound axial isothiocyanate (Cu(1)−N(3) 2.506(5) Å), which completes a nominal square-pyramidal coordination. The copper atom is displaced by 0.093 Å from the mean plane of the equatorial N_2O_2 donor set. However an additional longer axial contact from one of the secondary disordered alcoholic oxygens (O(2)) effectively completes a

(24) Downard, A. J.; McKee, V.; Tandon, S. S. *Inorg. Chim. Acta* **1990**, *173*, 181.

(25) Mandal, S. K.; Thompson, L. K.; Newlands, M. J.; Gabe, E. J.; Nag, K. *Inorg. Chem.* **1990**, *29*, 1324.

(26) Mandal, S. K.; Thompson, L. K.; Newlands, M. J.; Gabe, E. J. *Inorg. Chem.* **1989**, *28*, 3707.

(27) Mandal, S. K.; Thompson, L. K.; Nag, K.; Charland, J.-P.; Gabe, E. J. *Inorg. Chem.* **1987**, *26*, 391.

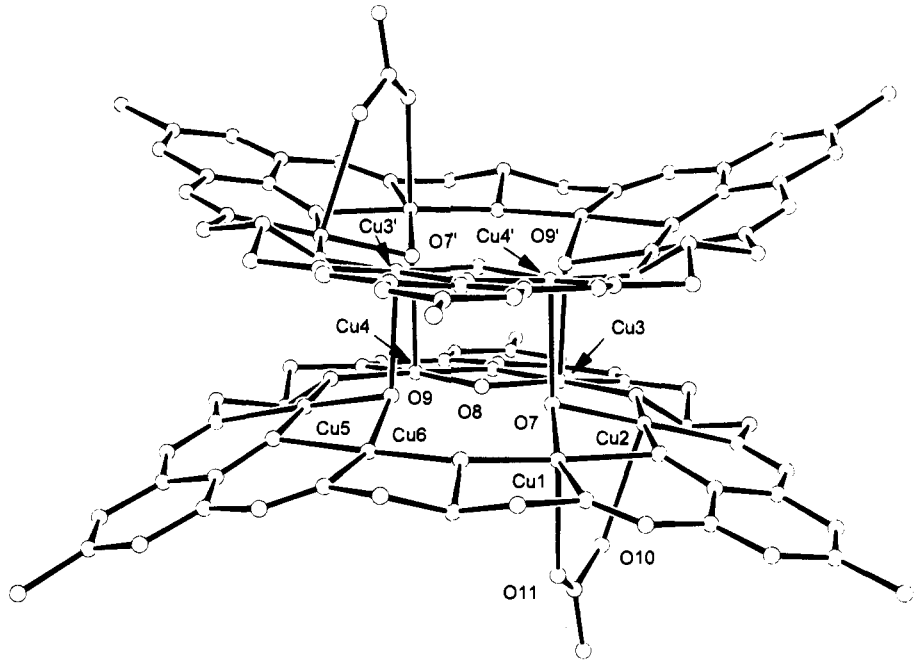

Figure 2. Structural representation depicting the dodecanuclear dimer in $[Cu_6(MME)(\mu_2\text{-}OH)_3]_2(NO_3)_6\cdot 10H_2O$ (**1**).

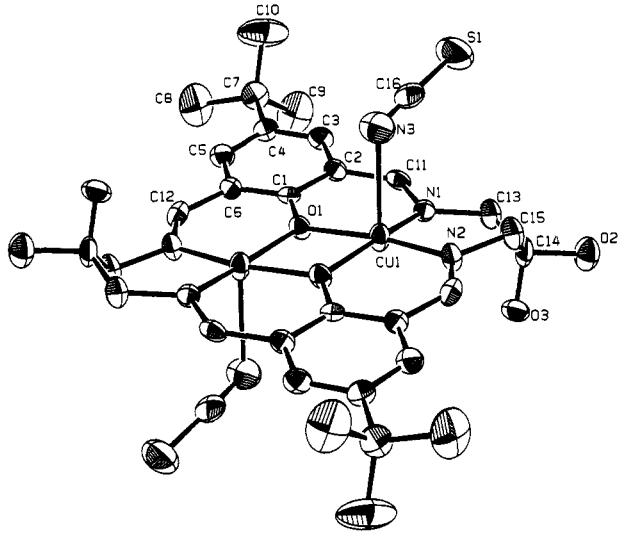

Figure 3. Structural representation for $[Cu_2(H_2MTB)(NCS)_2]_n$ (**6**), with hydrogen atoms omitted (50% probability thermal ellipsoids).

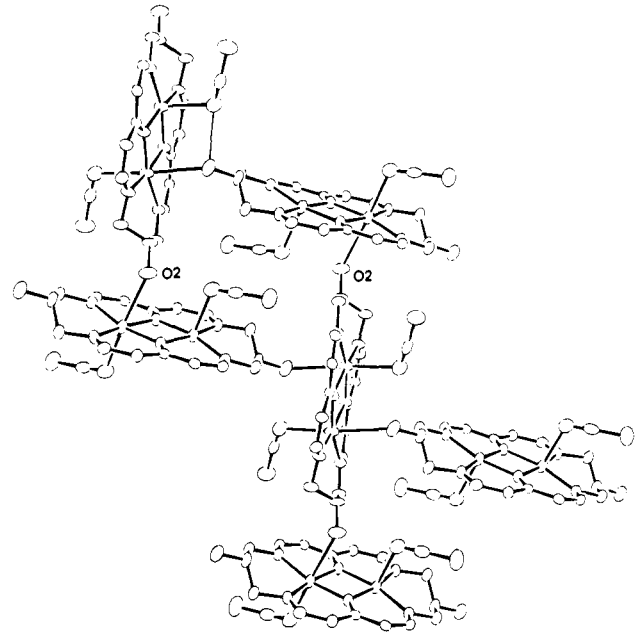

Figure 4. Extended structural representation for $[Cu_2(H_2MTB)(NCS)_2]_n$ (**6**).

distorted six-coordinate structure at each copper center and generates a rather complex 2-D extended structural arrangement, which is illustrated in Figure 4 (ligand *tert*-butyl groups omitted). Extended arrangements of this sort have been observed before for MME and MTB complexes with e.g. $[Cu_2Cl_4]^{2-}$ and $[Cu_2(N_3)_6]^{2-}$ fragments linking the binuclear centers together.[13]

Synthesis and Spectroscopic and Magnetic Properties. The 1,3-diamino-2-hydroxypropane fragment behaves like propanediamine in some template condensations with Mn, Ni, and Cu salts,[13,24] and the secondary alcoholic group does not coordinate. Six-membered chelate rings are formed in these complexes, with essentially planar binuclear centers in the nickel and copper complexes. In the syntheses of these complexes the copper salts were reacted with the appropriate diformylphenol, usually in methanol, followed by addition of DAHP and extended refluxing. In order to involve the secondary alcoholic group in coordination, considerable molecular rearrangement would be required, and also addition of base would seem essential. The use of NEt_3 in the present study was found to facilitate the deprotonation of the secondary alcohol and cause it to act as a donor. The condensation reaction forms five-membered chelate rings at the DAHP fragment, which clearly is the driving force for the formation of a 3:3 macrocyclic ring. There is no evidence for the formation of 2:2 macrocyclic complexes involving the incorporation of four metal centers. This behavior can be contrasted with comparable template condensations of DFMP and DFTBP with 1,5-diamino-3-hydroxypropane in the presence of copper(II) and manganese(II) salts, which form 2:2 tetranuclear macrocyclic fragments, but without the addition of base.[2,3,9,10] In these cases each chelate ring is six-membered. The formation of **6** from the mother liquor from the reaction used to prepare **4** indicates that the reactions contain an oligomeric mixture of 2:2 dinuclear and 3:3 hexanuclear macrocyclic species but that 2:2 tetranuclear species are less likely to form. The possibility of higher order oligomers should not be discounted, in view of the recent report

Table 4. Interatomic Distances (Å) and Angles (deg) Relevant to the Copper Coordination Spheres in $[Cu_6(MME)(\mu_2\text{-}OH)_3]_2(NO_3)_6\cdot 10H_2O$ (**1**)

Cu(1)−O(1)	1.98(1)	Cu(4)−O(3)	1.96(1)
Cu(1)−O(6)	1.91(1)	Cu(4)−O(4)	1.95(1)
Cu(1)−O(7)	1.96(1)	Cu(4)−O(8)	1.99(1)
Cu(1)−N(6)	1.94(2)	Cu(4)−N(3)	1.93(2)
Cu(2)−O(1)	1.96(1)	Cu(5)−O(4)	1.95(1)
Cu(2)−O(2)	1.93(1)	Cu(5)−O(5)	1.93(1)
Cu(2)−O(7)	1.94(1)	Cu(5)−O(9)	1.92(1)
Cu(2)−N(1)	1.93(2)	Cu(5)−N(4)	1.94(2)
Cu(3)−O(2)	1.96(1)	Cu(6)−O(5)	1.98(1)
Cu(3)−O(3)	1.97(1)	Cu(6)−O(6)	1.95(1)
Cu(3)−O(8)	1.98(1)	Cu(6)−O(9)	1.96(1)
Cu(3)−N(2)	1.96(2)	Cu(6)−N(5)	1.91(2)
Cu(1)−O(11)	2.37(2)	Cu(4)−O(18)	2.78(2)
Cu(2)−O(10)	2.58(2)	Cu(5)−O(13)	2.83(3)
Cu(2)−O(4)	2.89(1)	Cu(5)−O(2)	2.91(1)
Cu(3)−O(9)	2.45(1)	Cu(6)−O(14)	2.42(2)
Cu(3)−O(16)	2.55(2)	Cu(4)−O(7)	2.43(1)
O(7)−O(8)	2.86(2)	Cu(3)−Cu(4)	2.960(4)
O(8)−O(9)	2.86(1)	Cu(4)−Cu(5)	3.571(4)
O(7)−O(9)	3.12(2)	Cu(5)−Cu(6)	2.935(5)
Cu(1)−Cu(2)	2.927(3)	Cu(1)−Cu(6)	3.569(5)
Cu(2)−Cu(3)	3.547(5)	O(7)−O(9)	3.13(2)
O(7)−O(8)	2.86(2)	O(8)−O(9)	2.86(2)
O(1)−Cu(1)−O(6)	173.1(6)	O(3)−Cu(4)−O(8)	82.8(5)
O(1)−Cu(1)−O(7)	80.5(5)	O(3)−Cu(4)−N(3)	90.1(6)
O(1)−Cu(1)−N(6)	88.4(6)	O(4)−Cu(4)−O(8)	102.4(5)
O(6)−Cu(1)−O(7)	103.1(5)	O(4)−Cu(4)−N(3)	84.4(6)
O(6)−Cu(1)−N(6)	86.9(6)	O(8)−Cu(4)−N(3)	171.1(6)
O(7)−Cu(1)−N(6)	164.5(6)	O(4)−Cu(5)−O(5)	176.9(6)
O(1)−Cu(2)−O(2)	176.0(5)	O(4)−Cu(5)−O(9)	101.3(5)
O(1)−Cu(2)−O(7)	81.6(5)	O(4)−Cu(5)−N(4)	85.5(6)
O(1)−Cu(2)−N(1)	90.3(6)	O(5)−Cu(5)−O(9)	81.5(5)
O(2)−Cu(2)−O(7)	102.4(5)	O(5)−Cu(5)−N(4)	91.6(6)
O(2)−Cu(2)−N(1)	85.7(6)	O(9)−Cu(5)−N(4)	173.1(6)
O(7)−Cu(2)−N(1)	171.7(6)	O(5)−Cu(6)−O(6)	174.2(5)
O(2)−Cu(3)−O(3)	173.1(5)	O(5)−Cu(6)−O(9)	79.5(5)
O(2)−Cu(3)−O(8)	103.7(4)	O(5)−Cu(6)−N(5)	89.0(6)
O(2)−Cu(3)−N(2)	84.2(6)	O(6)−Cu(6)−O(9)	104.2(5)
O(3)−Cu(3)−O(8)	82.9(5)	O(6)−Cu(6)−N(5)	86.4(6)
O(3)−Cu(3)−N(2)	89.0(6)	O(9)−Cu(6)−N(5)	162.9(6)
O(8)−Cu(3)−N(2)	170.7(6)	Cu(3)−O(8)−Cu(4)	96.4(4)
O(3)−Cu(4)−O(4)	173.7(6)	Cu(4)−O(4)−Cu(5)	133.0(8)
Cu(1)−O(1)−Cu(2)	96.1(6)	Cu(5)−O(9)−Cu(6)	98.4(5)
Cu(1)−O(7)−Cu(2)	97.5(6)	Cu(5)−O(5)−Cu(6)	97.1(5)
Cu(2)−O(2)−Cu(3)	131.6(6)	Cu(1)−O(6)−Cu(6)	135.2(6)
Cu(3)−O(3)−Cu(4)	97.8(5)		

Table 5. Interatomic Distances (Å) and Angles (deg) Relevant to the Copper Coordination Spheres in $[Cu_2(H_2MTB)(NCS)_2]_n$ (**6**)

Cu(1)−Cu(1)	3.094(1)	Cu(1)−N(1)	1.971(4)
Cu(1)−O(1)	1.961(3)	Cu(1)−N(2)	1.936(4)
Cu(1)−O(1)	1.970(3)	Cu(1)−N(3)	2.506(5)
O(1)−Cu(1)−O(1)	76.2(2)	O(1)−Cu(1)−N(3)	99.8(2)
O(1)−Cu(1)−N(1)	93.6(2)	N(1)−Cu(1)−N(2)	97.5(2)
O(1)−Cu(1)−N(2)	168.5(2)	N(1)−Cu(1)−N(3)	89.5(2)
N(2)−Cu(1)−N(3)	91.5(2)	O(1)−Cu(1)−N(1)	166.3(2)
Cu(1)−O(1)−Cu(1)	103.8(2)	O(1)−Cu(1)−N(2)	92.4(2)
O(1)−Cu(1)−N(3)	91.7(2)		

of a 4:4 macrocyclic ligand from the template condensation of DFMP and 1,2-diaminoethane in the presence of magnesium salts.[28]

The distinction between 2:2 and 3:3 macrocycles of DAHP can be readily made by examining the infrared bands associated with the azomethine C=N group. In the 2:2 cases, a strong band is observed in the range 1620−1635 cm^{-1},[24] while for the 3:3 systems (Table 6), comparable bands occur in the range 1641−1657 cm^{-1}. Analytical data also confirm the formation of 3:3 derivatives. Perchlorate ν_3 bands for **2** and **4** are split slightly, indicating possible coordination or lattice symmetry effects. Mull transmittance electronic spectral data for the 3:3 copper complexes (Table 6) generally exhibit one broad absorption, with some minor splitting in **3**−**5**, in the visible region associated with square or square-pyramidal species. The general similarity of the infrared spectra for **1**−**5** and the demonstrated dodecanuclear nature for **1** and **4** would reasonably suggest that similar dimeric structures exist for **2**, **3**, and **5**. The presence of three visible bands for **6** is consistent with the low-symmetry six-coordinate copper centers.

The nickel complexes **7** and **8** exhibit three main absorptions in their mull transmittance electronic spectra (Table 6), which suggest the presence of pseudooctahedral species, with the splitting of the ν_2 band indicating a lower symmetry component. A sharp doublet in the infrared in the range 3280−3360 cm^{-1} for both **7** and **8** indicates the presence of coordinated water, while a broad absorption at higher energy indicates lattice water also. A sharp $\nu_3(ClO_4^-)$ band at 1101 cm^{-1} (**7**) indicates uncoordinated perchlorate, while a single $\nu_1 + \nu_4$ nitrate combination band for **8** at 1737 cm^{-1} indicates ionic nitrate. Given the ionic nature of the perchlorate in **7**, any nickel coligands would have to be water. Since six-coordinate nickel(II) centers are indicated from the electronic spectral data and since twelve waters would be required to complete the coordination spheres of six nickel(II) centers in a hexanuclear ring arrangement, it seems reasonable to propose a dodecanuclear structure for **7**, similar to **1**, involving four axial intermolecular contacts. Some of the nickel(II) centers would be expected to be five-coordinate in such a model but would probably not be revealed in the electronic spectral analysis. Exo-dimer sites would be occupied by water molecules. A similar structural arrangement could reasonably be proposed for **8**.

Room-temperature magnetic moments for the copper complexes (Table 6) are all $<1.5\ \mu_B$, indicative of antiferromagnetic coupling. For **7** and **8**, room-temperature magnetic moments (Table 6) are close to normal values for uncoupled high-spin Ni(II) centers. Variable-temperature magnetic susceptibility measurements were carried out on dried, powdered samples of compounds **1**, **2**, **4**, **6**, **7**, and **8** in the temperature range 4−305 K. **6** behaves as a typical dinuclear complex with strong antiferromagnetic coupling. A small sample was analyzed, and the data were fitted to the Bleaney−Bowers equation.[29] The best fit gave $g = 2.08(1)$, $-2J = 672(45)$ cm^{-1} (the weak sample response in the magnetometer prevented a more accurate assessment of J). The exchange coupling constant compares with other related 2:2 macrocyclic complexes.[25-27] For **1**, **2**, and **4**, χ vs temperature profiles exhibit broad maxima in the range 150−220 K (**1**, 150 K; **2**, 200 K; **4**, 220 K), followed by an increase of magnetic susceptibility at very low temperature (see Figures 5 and 6 for **1** and **4**, respectively). The temperature dependencies of the magnetic susceptibility of **7** and **8** are reported in Figures 7 and 8, respectively, in the χT vs T form. χT values for **7** rise to a maximum of 1.6 emu·K·mol^{-1} at 17.3 K, with decreasing temperature, followed by a sharp decrease down to 0.96 emu·K·mol^{-1} at 5.2 K, while for **8** a steady decrease from 1.24 emu·K·mol^{-1} at 298.9 K to 0.805 emu·K·mol^{-1} at 5.3 K was observed.

Due to the complexity of the molecular structure observed for **1**, a first attempt to reproduce its magnetic behavior was made by assuming that the system is dominated by the magnetic interaction within the ring containing the six copper(II) ions. As the metal ions are alternately connected by different bridges, the magnetic susceptibility was calculated by using an exchange

(28) Nanda, K. K.; Venkatsubramanian, K.; Majumdar, D.; Nag, K. *Inorg. Chem.* **1994**, *33*, 1581.

(29) Bleaney, B.; Bowers, K. D. *Proc. R. Soc. London* **1952**, *A214*, 451.

Table 6. Spectroscopic and Magnetic Data

compound	μ_{eff} (μ_B) (RT)	electronic data (nm)[a]	infrared data (cm^{-1})
$[Cu_6(MME)(\mu_2\text{-}OH)_3]_2(NO_3)_6\cdot 10H_2O$ (**1**)	1.42	375, 650	1649[b]
$[Cu_6(MME)(\mu_2\text{-}OH)_3]_2(ClO_4)_6\cdot 6H_2O$ (**2**)	1.25	375, 650	1641[b]
$[Cu_6(MME)(\mu_2\text{-}OH)_3]_2(BF_4)_6\cdot 8H_2O$ (**3**)	1.37	390, [665], 700, [814]	1650[b]
$[Cu_6(MTB)(\mu_2\text{-}OH)_3]_2(ClO_4)_6\cdot 8H_2O$ (**4**)	1.26	390, 645, 680	1651[b]
$[Cu_6(MTB)(\mu_2\text{-}OH)_3]_2(BF_4)_6\cdot 14H_2O$ (**5**)	1.46	370, 665, [930]	1650[b]
$[Cu_2(H_2MTB)(NCS)_2]_n$ (**6**)	0.77	365, 425, 655, 690, [830]	1637,[b] 2050, 2032 (ν(NCS))
$[Ni_6(MME)(\mu_2\text{-}OH)_3(H_2O)_6]_2(ClO_4)_6\cdot 4H_2O$ (**7**)	3.13	950(ν_1) [625], [745] (ν_2) 400(ν_3)	1649[b]
$[Ni_6(MME)(\mu_2\text{-}OH)_3(H_2O)_6]_2(NO_3)_6\cdot 16H_2O$ (**8**)	3.19	970 (ν_1) [600], 750 (ν_2) 420 (ν_3)	1649[b]

[a] Mull transmittance. [b] ν(C=N).

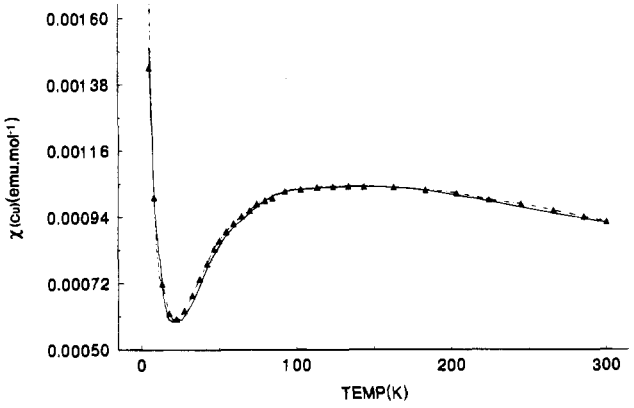

Figure 5. Temperature dependence of the magnetic susceptibility (Cu) for $[Cu_6(MME)(\mu_2\text{-}OH)_3]_2(NO_3)_6\cdot 10H_2O$ (**1**). The curves are calculated for $g = 2.05$ and $-2J_1 = -2J_2 = 318.4$ cm^{-1} using the six-spin model (dashed line) and for $g = 2.05$, $-2J_1 = 303.8$ cm^{-1}, $-2J_2 = 262.8$ cm^{-1}, and $-2J_3 = 20.0$ cm^{-1} for the twelve-spin model (full line) (1.91% monomeric impurity).

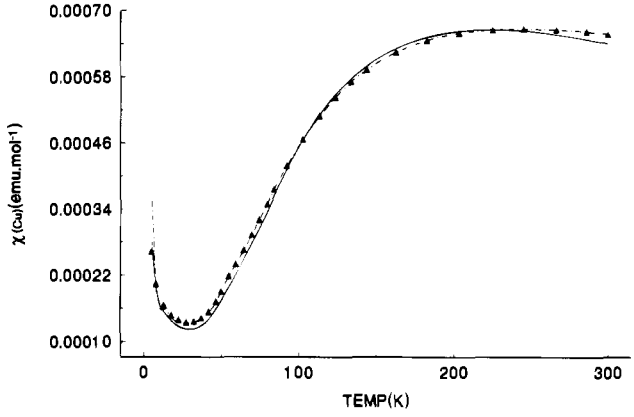

Figure 6. Temperature dependence of the magnetic susceptibility (Cu) $[Cu_6(MTB)(\mu_2\text{-}OH)_3]_2(ClO_4)_6\cdot 8H_2O$ (**4**). The curves are calculated for $g = 2.05$ and $-2J_1 = -2J_2 = 598.8$ cm^{-1} using the six-spin model (dashed line), and $g = 2.05$, $-2J_1 = 494.2$ cm^{-1}, $-2J_2 = 412.8$ cm^{-1}, and $-2J_3 = 16.4$ cm^{-1} for the twelve-spin model (full line) (0.34% monomeric impurity).

Hamiltonian where two different coupling constants were present ($\mathbf{H} = -2J_1S_i\cdot S_{i-1} - 2J_2S_i\cdot S_{i+1}$).[30] The χ values calculated at the end of the minimization procedure are in very good agreement with the experimental data (see Figure 5) ($f_{min} = \Sigma(\chi_{obs} - \chi_{calc})^2/\Sigma(\chi_{obs})^2$): the exchange coupling is antiferromagnetic in nature and the best fit gave two coupling constants with the same value, namely $-2J_1 = -2J_2 = 318.4$ cm^{-1}, with a small amount of a monomeric impurity (1.91%), which

(30) Pardi, L.; Gatteschi, D. *Gazz. Chim. Ital.* **1993**, *123*, 231.

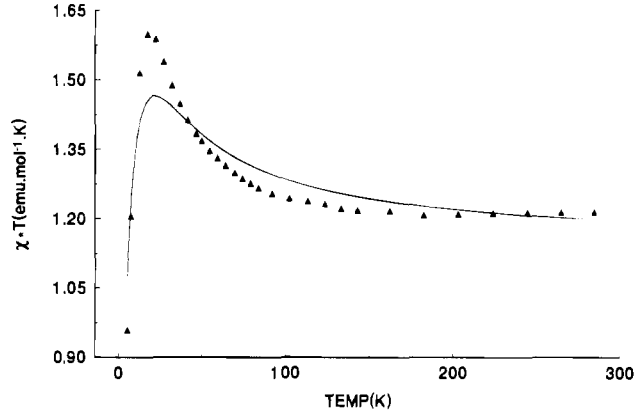

Figure 7. Temperature dependence of the χT values (Ni) for $[Ni_6(MME)(\mu_2\text{-}OH)_3(H_2O)_6]_2(ClO_4)_6\cdot 4H_2O$ (**7**). The curve is calculated for $g = 2.20$, $2J_1 = 31.4$ cm^{-1}, and $2J_2 = -3.0$ cm^{-1}.

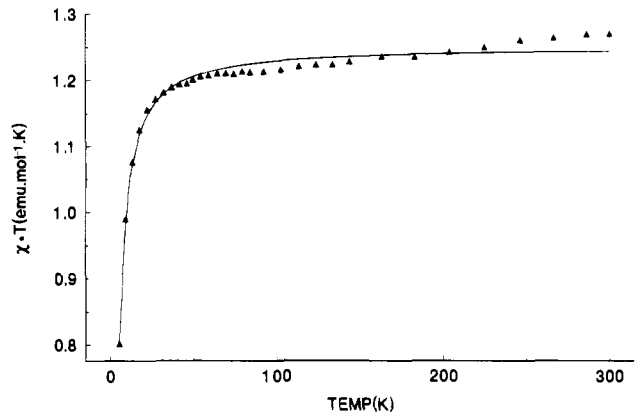

Figure 8. Temperature dependence of the χT values (Ni) for $[Ni_6(MME)(\mu_2\text{-}OH)_3(H_2O)_6]_2(NO_3)_6\cdot 16H_2O$ (**8**). The curve is calculated for $g = 2.20$, $2J_1 = 0.34$ cm^{-1}, and $2J_2 = -4.0$ cm^{-1}.

accounts for the increase in the χ values at low temperature. To check that this equality is not a computational artifact, the minimization procedure was repeated several times using different sets of starting values for the coupling constants, but all the attempts ended with the same values for J_i. Since the molecular structure of **4** is similar to that of **1**, the same model was applied to describe its magnetism, and the best fit to the observed magnetic susceptibility data gave again two coincident coupling constants with a value of $-2J_i$ of 598.8 cm^{-1}, with 0.34% of monomeric impurity. Again the equivalence of the two coupling constants was confirmed by several calculations.

It is not easy to justify these results on the basis of the structural features observed for **1** and **4**. The copper ions are alternately connected in the six-membered ring by bridging oxygen atoms which are chemically different, and each ion is linked with a single bridge to the copper ion on one side and

with a double bridge to the other metal. There are no well-developed magneto–structural correlations between Cu–O–Cu angles and coupling constants for phenoxide oxygens, but for alkoxide-bridged dicopper(II) complexes a reasonable correlation does exist,[31] which parallels the well-documented dihydroxy case,[32] and as a consequence very strong antiferromagnetic coupling might be anticipated through the alkoxide oxygens, considering the very large alkoxide bridge angles (131.6–135.2°) observed for **1**. The hydroxide bridge angles (average 97.4°) are very close to the critical angle for accidental orthogonality established by Hatfield for the dihydroxide system,[32] and so a very weak antiferromagnetic or possibly ferromagnetic contribution might be anticipated. The average phenoxide angle (97.0°) would be expected to be responsible for quite strong antiferromagnetic exchange ($-2J \approx 600$ cm^{-1}).[33] The preliminary structure of **4** indicates comparable alkoxide bridge angles but somewhat larger hydroxide and phenoxide angles, which is consistent with the larger $-J$ values. Given the circumstances, it is difficult to believe that this complex situation yields equivalent exchange interactions and that they are relatively small. It is probably more reasonable to suspect an inadequacy in the coupling scheme used to model the magnetic behavior of the system.

Actually each ring is connected to an adjacent ring through two hydroxide oxygens (O(7) and O(9)), which are bonded to two copper ions belonging to a different macrocycle, which leads to four such contacts between the rings (Figure 2). Despite the fact that the intermolecular Cu–O distances are fairly long (≈2.44 Å), they are reasonable for axial interactions with copper, and it is possible that some exchange mechanism is operative via these bridges. Therefore an attempt was made to fit the magnetic susceptibility to a model with 12 copper(II) centers arranged in two equivalent rings, with alternating coupling constants ($-2J_1$ and $-2J_2$) and with the two rings coupled through four equivalent magnetic interactions ($-2J_3$). Due to the complexity of the system, it was not possible to apply a minimization procedure, and a trial and error method was used to find a fit to the experimental data. The final results for **1** and **4** are reported in Figures 5 and 6, respectively. The best fit parameters are $-2J_1 = 303.8$ cm^{-1}, $-2J_2 = 262.8$ cm^{-1}, and $-2J_3 = 20.0$ cm^{-1} (**1**) and $-2J_1 = 494.2$ cm^{-1}, $-2J_2 = 412.8$ cm^{-1}, and $-2J_3 = 16.4$ cm^{-1} (**4**). For all the calculations the g value was kept constant at 2.05 and a contribution due to the percentage of monomeric impurity calculated with the previous model for each complex was added. Actually, the quality of the final fits is not quite as good as those obtained with the simpler model, but the largest deviations are observed in the zone of the minima where the amount of monomeric impurity, which in these calculation was not a free parameter, plays a more significant role. In any case, the final sets of parameters derived with the more complex coupling scheme are considered more appropriate to describe the magnetic interactions in these complexes on the basis of their molecular structure. A similar data analysis for **2** gave $-2J_1 = -2J_2 = 485.2$ cm^{-1} ($g = 2.00$) for the six-spin model and $-2J_1 = 484.5$ cm^{-1}, $-2J_2 = 479.0$ cm^{-1}, and $-2J_3 = 16.4$ cm^{-1} ($g = 2.00$, 0.0355% monomeric impurity) for the twelve-spin model, for which the fit was slightly better. This lends support to a similar dodecanuclear structure for **2**.

The intra-ring $-2J_i$ values determined for **1**, **2**, and **4** are equivalent using the six-spin model and comparable using the twelve-spin model. However, given the very large alkoxide bridge angles for **1** and **4**, it is surprising that net exchange is not more strongly antiferromagnetic. The sums of the angles around the alkoxide oxygens fall in the range 349–352° (**1**), leading to a slight pyramidal distortion at each bridge. This might cause some reduction in exchange, but perhaps not enough to lead to such low values. Equally, distortions at the phenoxide bridges are small, with the sums of the oxygen angles falling in the range 352–360°, and so would not be expected to diminish antiferromagnetic coupling significantly. The inter-ring exchange couplings for **1**, **2**, and **4** are all relatively small ($-2J_3 = 16–20$ cm^{-1}), and although each axial bridge might not be expected to individually cause significant charge delocalization between the rings, four operating together might reduce intra-ring exchange substantially. The general similarity in the magnetic properties of **1**, **2**, and **4**, with smaller than expected intra-ring exchange and significant inter-ring exchange, supports the validity of the twelve-spin model. However, since this exchange model includes both types of intra-ring bridging interaction, the comparable nature of J_1 and J_2 may indicate some charge delocalization within the rings beyond just immediate local pairs.

On the assumption that the nickel derivatives have a structure similar to those of the copper analogues, the same strategy used for the Cu(II) derivatives was employed to analyze the magnetic structure of these compounds. A fit of the magnetic data for **7** and **8** was carried out using the model based on isolated six-membered rings. The final agreement between calculated and experimental data is not very satisfactory for **7**, but fairly good for **8**, as shown in Figures 7 and 8, respectively. The calculations gave slightly different parameters for the two compounds: $2J_1 = 31.4$ cm^{-1}, $2J_2 = -3.0$ cm^{-1} (**7**); $2J_1 = 0.34$ cm^{-1}, $2J_2 = -4.0$ cm^{-1} (**8**). For all the calculations the g value was kept constant at 2.20, and no correction was made for the presence of monomeric impurity. For both complexes, the best fit parameters indicate that both ferromagnetic and antiferromagnetic exchange mechanisms are operative, with coupling constants similar to those reported in analogous dinickel(II) and dodecanickel(II) derivatives.[34,35] For **7** it is apparent that the ferromagnetic term dominates, while for **8** the net exchange is antiferromagnetic. Unfortunately, it is not possible to improve the quality of the fits by using the model with interacting rings, since in this coupling scheme 12 spins with $S = 1$ would have to be included. To reproduce the magnetic properties, calculation of the energies of spin states ranging from $S = 0$ to 12, with the diagonalization of matrixes as large as 15 026 for $S = 2$, would be required, which is beyond our current computational capability. Further, it is not possible to reduce the dimensions of these huge matrixes by means of the symmetry[36] of the systems, since their actual structure is unknown. In addition, the lack of structural data does not reveal any correlation between the structural features of the molecules and the exchange mechanism. However the inadequacy of the simpler model for the nickel derivatives seems to support the suggestion of the similarity in the molecular structure between the nickel and copper complexes.

Conclusion

Dodecanuclear copper(II) complexes of 3:3 macrocyclic ligands, derived by the template condensation of 2,6-di-

(31) Merz, L.; Haase, W. *J. Chem. Soc., Dalton Trans.* **1980**, 875.
(32) Crawford, V. H.; Richardson, H. W.; Wasson, J. R.; Hodgson, D. J.; Hatfield, W. E. *Inorg. Chem.* **1976**, *15*, 2107.
(33) Thompson, L. K.; Mandal, S. K.; Tandon, S. S.; Bridson, J. N.; Park, M. K. Unpublished results.
(34) Nanda, K. K.; Thompson, L. K.; Bridson, J. N.; Nag, K. *J. Chem. Soc., Chem. Commun.* **1994**, 1337.
(35) Blake, A. J.; Grant, C. M.; Parsons, S.; Rawson, J. M.; Winpenny, R. E. P. *J. Chem. Soc., Chem. Commun.* **1994**, 2363.
(36) Delfs, C.; Gatteschi, D.; Pardi, L.; Sessoli, R.; Wieghardt, K.; Hanke, D. *Inorg. Chem.* **1993**, *32*, 3099.

formylphenols with 1,3-diamino-2-hydroxypropane, consist of hexagonal cyclic arrays of metal centers linked axially through hydroxide bridges. The variable-temperature magnetic properties have been interpreted using both six- and twelve-spin cluster models, and successful data fits have been obtained with three antiferromagnetic exchange interactions, two occurring within the rings and one between the metallacyclic rings. The generally reduced intra-ring antiferromagnetic exchange can be associated with a significant inter-ring antiferromagnetic exchange interaction through four axial bridging contacts.

Acknowledgment. We thank the Natural Sciences and Engineering Research Council of Canada (L.K.T.) and the Italian MURST and CNR (C.B.) for financial support for this study.

Supporting Information Available: Descriptions of the X-ray experimental procedures and tables listing detailed crystallographic data, hydrogen atom positional parameters, anisotropic thermal parameters, and bond lengths and angles (33 pages). Ordering information is given on any current masthead page.

IC9502178